High resolution detection system for time of flight electron spectrometry

A.S. Tremsin[1,*], G.V. Lebedev[2], O.H.W. Siegmund[1], J.V. Vallerga[1],

J.B. McPhate[1], Z. Hussain[2]

[1]Space Sciences Laboratory, University of California at Berkeley

Berkeley, CA 94720, USA

[2]Advanced Light Source, Lawrence Berkeley National Laboratory, Berkeley, CA 94720,

USA

Abstract

One of the key components of a time of flight (TOF) spectrometer is the detection system. In addition to high timing resolution, accurate 2-dimensional imaging substantially broadens the areas of applications of TOF spectrometers; for example, add a new dimension to angle-resolved photoemission spectroscopy (ARPES).

In this paper we report on the recent developments of a high spatial (<50 μm) and timing (<130 ps) resolution imaging system capable of selective detection of electrons, ions and/or photons. Relative to our previously reported results, we have substantially improved the counting rate capabilities of the system especially for cases where the energy range of interest represents a small fraction of the incoming flux at the detector

* Corresponding author.
E-mail address: ast@ssl.berkeley.edu (A.S. Tremsin)

plane. The new system ignores all the events outside of a tunable time window substantially decreasing the dead time required for the event processing. That allows high resolution TOF measurements within a given energy or momentum range and also can be used for distinguishing (or disabling) detection of photons versus detection of charged particles. The counting rate within a given energy window can be as high as ~400 KHz at 10% dead time.

The electron detection system reported in the paper was developed for the TOF ARPES experiments at the Advanced Light Source, Lawrence Berkeley National Laboratory

PACS: 29.40.-n; 07.85.Qe; 33.60.-q; 79.60.-I;

Keywords: Photoemission electron spectrometry; Event counting detectors; High spatial and temporal resolution, Synchrotron instrumentation

1. Introduction

New experimental techniques developed over last decade enable studies of correlated interplay between atomic and electronic structure in complex materials such as high temperature superconductors, manganites and many others. Some exotic phenomena in those materials arise from the strong interaction between charge, spin, orbital and vibrational degrees of freedom. The anisotropic nature of these interactions demands very accurate measurements of electron momentum, in addition to high spectral resolution. Currently a widely used technique for the investigation of static electronic properties of

strongly correlated systems is high resolution angle-resolved photoemission spectroscopy (ARPES) [1]. However, most ARPES experiments only allow studies of static phenomena as they have either relatively poor energy or poor angular resolution. A new system developed at Lawrence Berkeley Laboratory, which has both high energy and high momentum resolution, should allow studies of dynamic phenomena [2]. One of the key elements of this system is a high resolution detector capable of registering both XY position (converted into 2D momentum) and timing, T (used to calculate the energy), of photoelectrons arriving at the detection plane [3]. In this paper we describe the performance of our current detection system and optimization of its counting rate capabilities with respect to the signal of interest.

2.Detection system

Our event counting detection system is capable of measuring simultaneously the 2D position of an incoming electron/photon/ion and the timing of its arrival at the detector plane. At the front of the detector is a 90% transmissive mesh, the potential of which can be varied allowing for selective detection of positively or negatively charged particles. A stack of microchannel plates positioned ~1mm behind the input mesh is used for the electron amplification with factor of 10^6-10^7. The amplified signal is finally collected by a cross delay line (XDL) readout, the output of which is capacitively coupled to associated electronics for encoding of the 2D position of an event and its timing. Each event requires ~0.6 μs to process, resulting in 10% dead time at an input rate of ~0.4 MHz. The detector active area is 25 mm in diameter. A more detailed description of this particular detector and MCP detection technology in general can be found in references [3]-[7].

Fig. 1 shows an image obtained with our detection system under full field UV illumination, while Fig. 2 shows an image obtained with electrons from an electron gun and a cross section through it. The spatial resolution of the detection system was measured to be better than 50 μm FWHM with timing accuracy better than 130 ps FWHM [3]. The linearity of the timing channel is shown in Fig. 3, where the distance between each consecutive peak is very close to the ideal 10 ns value. Spatial and temporal information for each detected event allows dynamic imaging (in particular in momentum space) for a given energy range/ranges, as demonstrated by our first experimental evaluation of the system at a synchrotron beam [3].

3. Optimization of counting rate capabilities

Most event-counting detection systems are impaired by a dead time – time required for processing of an individual event. That drawback becomes debilitating for the experiments where unwanted signals dominate the incoming flux (e.g., a bright prompt photon peak from a synchrotron beam versus a weak delayed photoemission or photoelectron flux). In this case the effective count rate (number of useful events per second) may become very small and a long data acquisition will be necessary in order to obtain reasonable statistics. The ideal detection system would completely ignore the unwanted events and process only those of interest.

We optimized our detection system and implemented an "enable" signal, which determines which events are to be processed. The selection of useful events can be done both by an energy range (acceptable time of flight) or by allowed momentum space

(position on the detector). Fig. 4 illustrates an example of input enabled by the gate (channel 2, active low). All the events outside of the enable gate are ignored and do not trigger the data acquisition system. This is much more efficient than the previously used scheme of post-detection software elimination of unwanted signals, in which the detector had to process an event before making a decision. An example of an experiment where our optimization can be very useful is shown in Fig. 5. This timing histogram has two photon peaks: a prompt photon peak from a synchrotron beam and a 50 ns delayed photon peak comprising only ~5% of total incoming flux. In that case disabling all the time delays outside of the range of interest (measured from the synchrotron trigger) allows an improvement in operational efficiency of up to 20 times, substantially decreasing data acquisition time. With this optimization our detection system can operate at ~0.4 MHz counting rates for a *specific range* of incoming energies (TOF) or angles (event position).

4. References

[1] A. Damascelli, Physica Scripta., "Probing the Electronic Structure of Complex Systems by ARPES" Vol. T109, 61-74, 2004

[2] G. V. Lebedev, Z. Hussain, C. Jozwiak and N. Andresen, "TOF Electron Energy Analyzer for Spin and Angular Resolved Photoemission Spectroscopy", Proc of 7th International Conference on Charged Particle Optics, Cambridge, July 2006, to be published in Nucl. Instr. and Meth. **A.**

[3] A.S. Tremsin, G.V. Lebedev, O.H.W. Siegmund, J.V. Vallerga, J.S. Hull, J.B. McPhate, C. Jozwiak, Y. Chen, J.H. Guo, Z.X. Shen, Z. Hussain, "High spatial and temporal resolution photon/electron counting detector for synchrotron radiation research", Proc. IMAGING 2006, Stockholm, June 2006, to be published in Nucl. Instr. Meth. A.

[4] G. W. Fraser, "Imaging in astrophysics (and elsewhere)", Nucl. Instr. Meth. A 471 pp.170-173 (2001).

[5] O. H.W. Siegmund, J.V. Vallerga, J. McPhate and A.S. Tremsin, "Next generation microchannel plate detector technologies for UV Astronomy", Proc. SPIE vol. 5488 "UV-Gamma Ray Space Telescope Systems", Glasgow, June 2004, pp.789-800 (2004).

[6] O. H. W. Siegmund , B. Y. Welsh, J. V. Vallerga, A. S. Tremsin, J. B. McPhate, „High-performance microchannel plate imaging photon counters for spaceborne sensing", Proc. SPIE vol. 6220, "Spaceborne Sensors III", Orlando, Florida, May pp.53-64, 2006.

[7] A. S. Tremsin, O. H. W. Siegmund, J. V. Vallerga, J. Hull, "Cross Strip Readouts for Photon Counting Detectors with High Spatial and Temporal Resolution", IEEE Trans. Nucl. Sci.. 51 pp.1707-1711 (2004).

5. Figure captions

Fig. 1. A full field illumination image obtained with UV photons from a mercury vapor penray lamp. A shadow of the input mesh is seen on the image. The detector modal gain was ~$6x10^6$.

Fig. 2. (a) An image of a beam of electrons emitted by a gun with short duration pulses (~100 ps). The shadow of the input mesh with 25 μm wires on 250 μm centers is seen on the image. **(b)** Cross section through the image indicating that detector spatial resolution is better than 50 μm FWHM.

Fig. 3. A time histogram of detected photoelectron events illustrating the linearity of timing resolution. Laser driven photoelectron source operated at a 100 MHz rate producing photoelectrons at time bins separated by 10 ns.

Fig. 4. A snapshot of the scope showing photon signals (channel 1) and enable gate (channel 2). The events outside of the gate-enabled timing (shaded area) are ignored by the processing electronics, which is triggered only on the events within the given ~15 ns timing range. The detector dead time is greatly reduced for the experiments where the signal of interest constitutes only a small fraction of total flux at the detector plane.

Fig. 5. Time histogram of detected photon events. Note the logarithmic scale on the y-axis. The signal of interest (only 5% of total flux) is the second peak delayed by ~50 ns relative to the dominant prompt photons. Disabling all the events in the shaded area by gating the detector substantially improves the detection efficiency for the useful signal.

Fig. 1

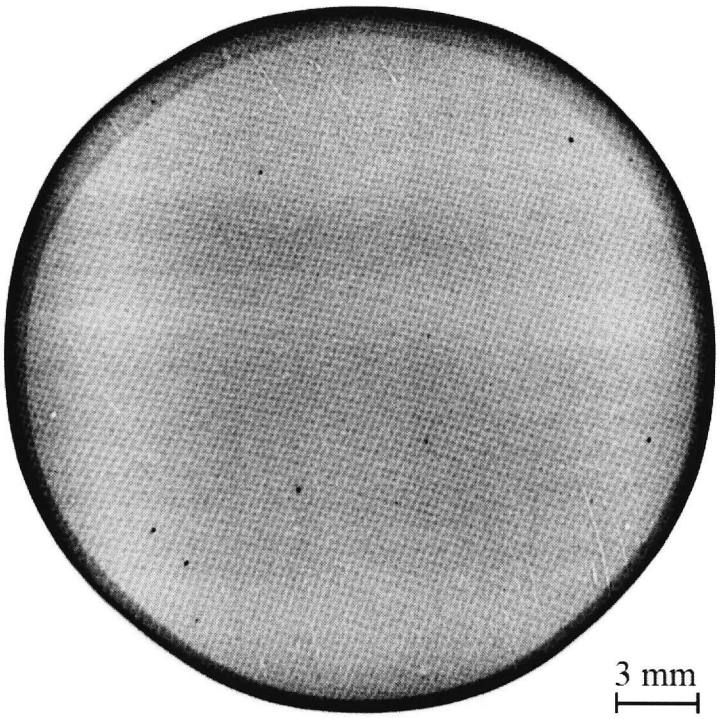

Fig. 2.a

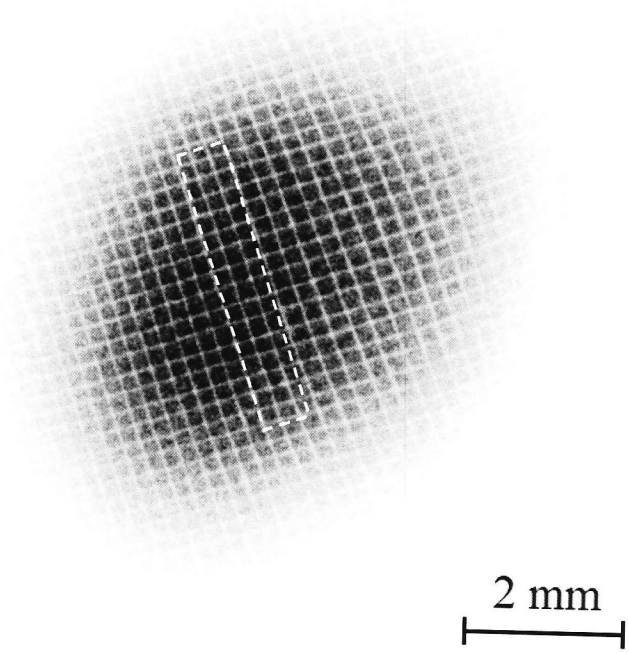

Fig. 2.b

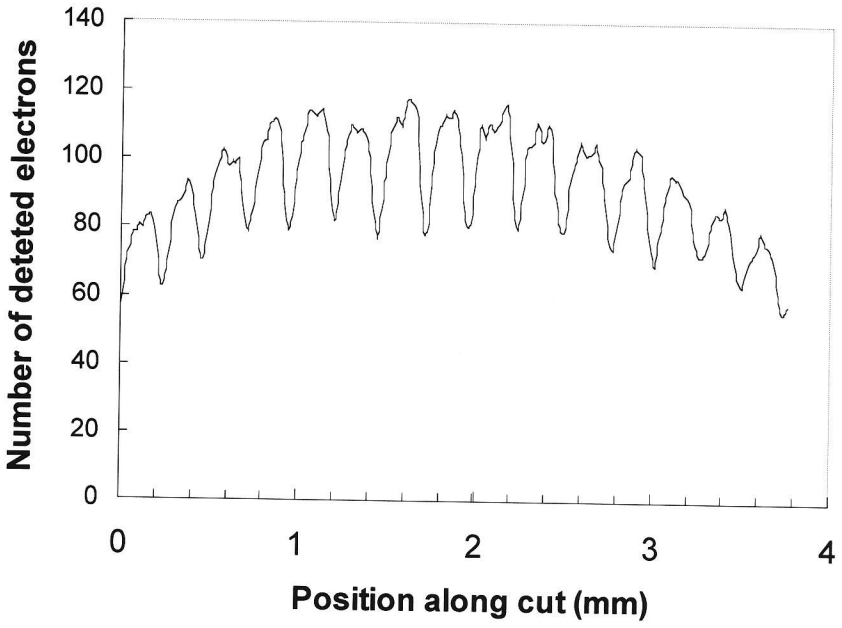
Number of deteted electrons
140
120
100
80
60
40
20
0
0
1
2
3
4
Position along cut (mm)

Fig. 3

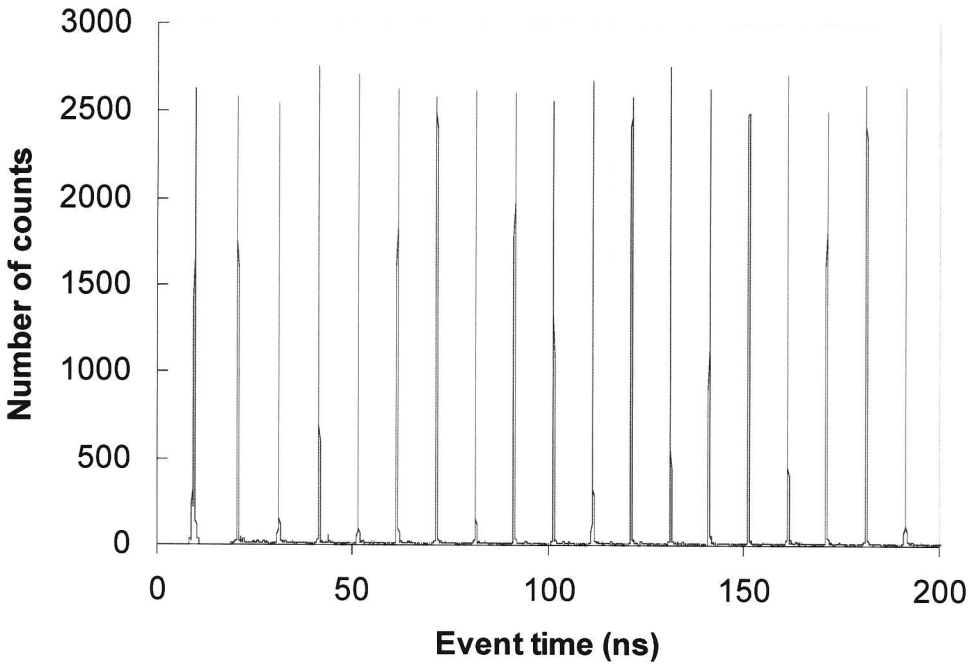
3000
2500
2000
1500
1000
500
0
Number of counts
0
50
100
150
200
Event time (ns)

Fig. 4

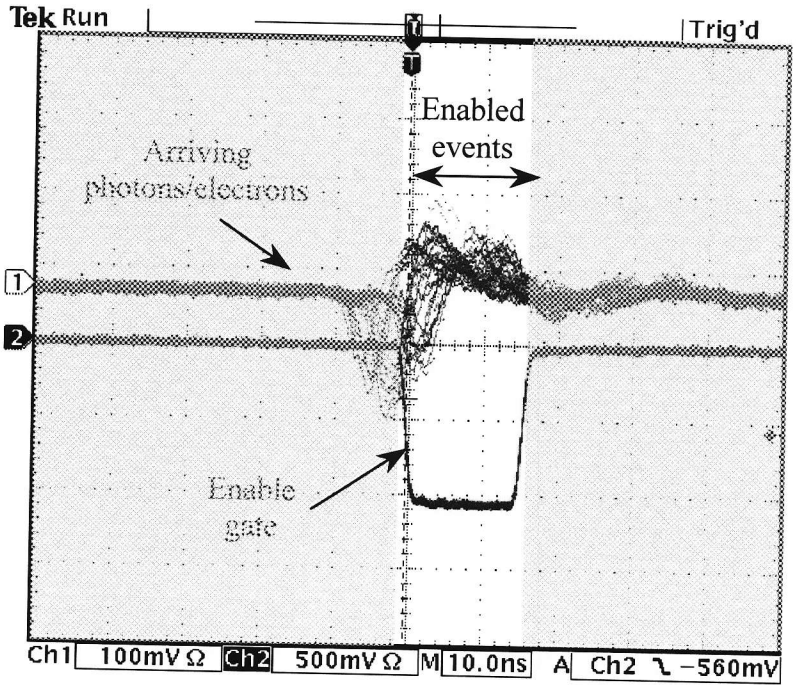
Tek Run
Trig'd
Enabled
events
Arriving
photons/electrons
1
2
Enable
gate
Ch1 100mV Ω
Ch2 500mV Ω
M 10.0ns
A Ch2 ↘ -560mV

Fig. 5